

## **Final Report**

**Development of large capacity Lead-Carbon Hybrid Ultracapacitors for  
energy harvesting and storage**

**A K Shukla**

**Solid State & Structural Chemistry Unit**

**Indian Institute of Science, Bangalore**

**July 2012**

## Report Documentation Page

*Form Approved*  
OMB No. 0704-0188

Public reporting burden for the collection of information is estimated to average 1 hour per response, including the time for reviewing instructions, searching existing data sources, gathering and maintaining the data needed, and completing and reviewing the collection of information. Send comments regarding this burden estimate or any other aspect of this collection of information, including suggestions for reducing this burden, to Washington Headquarters Services, Directorate for Information Operations and Reports, 1215 Jefferson Davis Highway, Suite 1204, Arlington VA 22202-4302. Respondents should be aware that notwithstanding any other provision of law, no person shall be subject to a penalty for failing to comply with a collection of information if it does not display a currently valid OMB control number.

1. REPORT DATE <b>26 AUG 2012</b>	2. REPORT TYPE <b>Final</b>	3. DATES COVERED <b>18-04-2011 to 17-04-2012</b>	
4. TITLE AND SUBTITLE <b>Development of large capacity PbO<sub>2</sub>-Carbon hybrid ultracapacitors for energy storage</b>		5a. CONTRACT NUMBER	
		5b. GRANT NUMBER	
		5c. PROGRAM ELEMENT NUMBER	
6. AUTHOR(S) <b>Ashok Kumar Shukla</b>		5d. PROJECT NUMBER	
		5e. TASK NUMBER	
		5f. WORK UNIT NUMBER	
7. PERFORMING ORGANIZATION NAME(S) AND ADDRESS(ES) <b>Indian Institute of Science, Science Institute PO, Bangalore 560012, India, IN, 560012</b>		8. PERFORMING ORGANIZATION REPORT NUMBER <b>N/A</b>	
9. SPONSORING/MONITORING AGENCY NAME(S) AND ADDRESS(ES) <b>AOARD, UNIT 45002, APO, AP, 96338-5002</b>		10. SPONSOR/MONITOR'S ACRONYM(S) <b>AOARD</b>	
		11. SPONSOR/MONITOR'S REPORT NUMBER(S) <b>AOARD-114034</b>	
12. DISTRIBUTION/AVAILABILITY STATEMENT <b>Approved for public release; distribution unlimited</b>			
13. SUPPLEMENTARY NOTES			
14. ABSTRACT <b>Hybrid ultracapacitors (HUCs) are a new class of emerging electrochemical energy storage devices. Among various hybrid ultracapacitors, PbO<sub>2</sub> / Activated Carbon is an attractive system owing to its high cell voltage that provides it both high energy and power densities. In this project, we have designed and developed 12V / kF-range Lead-Carbon (LC) HUCs with absorbent-glass-mat (AGM) and silica-gel electrolyte configurations and tested their performance. The capacitance for the HUC in silica gel electrolyte configuration is found to be higher than AGM configuration because the enhancement of active surface area of positive plate and the effect of polymeric structure of silica gel on negative plate. The constant-power discharge curves show that lead-carbon HUCs have the capability to deliver energy as well as power for specified time duration. This dual feature of energy and power is a clear advantage of having a battery type electrode and a capacitor type electrode.</b>			
15. SUBJECT TERMS <b>ultra capacitors, ultra capacitors, power storage, power storage, Magneto-optical imaging , Magneto-optical imaging , lead oxide activated carbon</b>			
16. SECURITY CLASSIFICATION OF:			17. LIMITATION OF ABSTRACT <b>Same as Report (SAR)</b>
a. REPORT <b>unclassified</b>	b. ABSTRACT <b>unclassified</b>	c. THIS PAGE <b>unclassified</b>	
			18. NUMBER OF PAGES <b>19</b>
			19a. NAME OF RESPONSIBLE PERSON



. In this project, we have designed and developed 12V / kF-range Lead-Carbon (LC) HUCs with absorbent-glass-mat (AGM) and silica-gel electrolyte configurations as shown in Fig. 1 and have performance tested them.

Details on preparation of electrical double-layer carbon electrodes, substrate-integrated PbO<sub>2</sub> (referred as Lead) electrodes, and assembly of lead-carbon ultracapacitor devices are given below.

#### *Preparation of activated-carbon electrodes*

5 wt. % of Poly(vinylidene fluoride) (PVDF) polymer was dissolved in required quantity of Dimethylformamide (DMF) solvent by ultrasonication for 15 mins. Subsequently, 85 wt. % of high surface area (~1512 m<sup>2</sup>/g) amorphous carbon (Meadwestvaco carbon X-090177) and 10 wt. % of activated charcoal AR (~ 974 m<sup>2</sup>/g) (s d fine-chem Ltd., Mumbai-400030, India) were dispersed into the PVDF-DMF solution to obtain a thick carbon-ink which was applied onto 1 mm thin graphite sheets with geometrical area was of 172.5 (11.5 cm x 15 cm) sq. cm and the tag dimensions were of 1.5 cm x 1.5 cm x 1 mm. Weight of the graphite electrode was ~ 40 g. Each side of the graphite current collector was contained by ~ 3 g carbon. Graphite electrodes were subsequently dried in an air oven at 80 °C for 6-8 h.

#### *Preparation of substrate-integrated PbO<sub>2</sub> (Lead) electrodes*

Substrate-integrated PbO<sub>2</sub> electrodes were prepared from lead sheets (99.9% purity) of dimensions 11.5 cm x 15 cm x 0.3 mm with tag dimension of 1.5 cm x 1.5 cm x 0.3 mm weighing ~ 90 g. Lead sulphate formed on the lead sheets after overnight dipping in 6 M aq. H<sub>2</sub>SO<sub>4</sub> was converted to PbO<sub>2</sub> by constant-current charging at 1 mA cm<sup>-1</sup>. Five consecutive charge-discharge cycles at 1 mA cm<sup>-1</sup> provided the capacity of Substrate-integrated PbO<sub>2</sub>

electrodes were  $1 \text{ mAh cm}^{-1}$ . These electrochemically formed Substrate-integrated  $\text{PbO}_2$  electrodes were used as positive plates in HUCs.

#### *Assembly of 12 V / kF- range HUC*

12 V HUCs with activated carbon electrodes sandwiched between substrate-integrated  $\text{PbO}_2$  electrodes were assembled in AGM configuration in 6 M aq. sulphuric acid or silica gel with 1.4 g/cc aq. sulphuric acid using a commercial six-compartment 12 V/ 42 Ah lead-acid battery containers. Accordingly, HUCs comprised six hybrid ultracapacitors with appropriate number of electrodes connected in series. Each compartment was containing seven positive plates and six negative plates in parallel connection. Capacitors unit were filled by absorbent-glass-mat (AGM) soaked with adequate aq.  $\text{H}_2\text{SO}_4$  electrolyte, or silica gel-electrolyte. The weights of two devices are  $\sim 10$  kg. HUCs were performance tested using a Bitrode instrument fitted with a LCN-Power Module. A. C. impedance studies were carried out by using Autolab Potentiostat/Galvanostat-Model 30 in conjunction with a voltage multiplier.

#### *Constant current charge-discharge testing*

12 V HUCs were performance tested by constant current charge-discharge at varying currents. Two ranges of current value was selected, lower range values like 3, 6, 9, 12, 15 A and higher range values like 25, 50, 75, 100 A. Each cases capacitance values (C) were calculated from the ratio of negative slopes of discharge profiles and the corresponding currents. From the basic understanding one can write,  $Q = C \times V$ , where Q is the charge on the electrodes and V is the voltage difference between the electrodes. Since  $Q = I \times t$ , where I and t represent current and time, respectively. Accordingly,  $V = \frac{I \times t}{C}$ , and by differentiating with respect to time at constant current, we get,  $\frac{dV}{dt} = \frac{I}{C}$ . During the constant current charge-discharge of HUCs, voltage varies almost linearly with time. The charging profiles have

positive slope of  $I/C$  while discharge profiles have negative slope of  $-I/C$ . In practical situation, during the discharge of HUCs, there will be an initial voltage drop due to the internal ohmic resistance, called as IR drop, where R is the ohmic resistance. Since this IR drop is not feasible for capacitive discharge, the capacitance values were calculated excluding both ESR (equivalent series resistance) and EDR (electrical double-layer resistance).

In this study HUCs were subjected to constant currents charge to a cut-of-voltage of 13.8 V followed by potentiostatic charge at 13.8 V for 1 h. Then constant currents discharge up to 6 V. The capacitance values at 3 A current (C-rate for the positive electrode) are 1.38 kF and 2.45 kF which decrease to 1.25 kF and 2.31 kF at a discharge current of 15 A (5-C rate for the positive electrode) for AGM and silica gel electrolyte configurations, respectively. At the higher current values (e.g. 25, 50, 75, 100 A) capacitance again decreases. All of the discharge profiles of HUCs at constant currents are shown in Fig. 2 (a, b) and 3 (a, b). The capacitance for the HUC in silica gel electrolyte configuration is found to be higher than AGM configuration because the enhancement of active surface area of positive plate and the effect of polymeric structure of silica gel on negative plate.

#### *Temperature dependence of capacitance*

The trend for change in the capacitance values at varying temperatures are different for AGM and silica gel HUCs as shown in Fig. 4 (a, b). The capacitance is found to decline with decreasing temperature, due to the lowering of electrolyte conductivity and freezing of electrolyte below zero degrees centigrade. The working temperature range of HUC is too wide from -30 to 50 °C that it can be used at any feasible environment.

### *Faradaic efficiency determination*

Faradaic efficiencies of HUCs, AGM and silica gel electrolyte configuration, were calculated from constant current charge-discharge at 3A current. From Fig 5 the efficiency values are indicated as 93 % and 92 % for AGM and gelled electrolyte HUC respectively. The high faradaic efficiency is achieved mainly for using activated carbon capacitor electrode as negative plates and this is one of the attractive features of the Substrate-integrated lead-carbon hybrid ultracapacitors.

### *Constant power discharge data*

Constant-power discharge curves at 10, 20, 30, 40 and 50 W for 12 V lead-carbon HUCs are shown in Fig.6 (a, b). HUCs were first charged by constant current at 0.3A up to a cut-of-voltage of 13.8 V followed by 1 h potentiostatic charging at 13.8 V. During the constant-power discharge of the HUCs, the current is found to increase as the voltage decreases. The constant-power discharge curves show that lead-carbon HUCs have the capability to deliver energy as well as power for specified time duration. This dual feature of energy and power is a clear advantage of having a battery type electrode and a capacitor type electrode.

### *Impedance study*

Internal resistance measurements have been done using A. C. impedance spectroscopy at different state-of-charge (at different voltage) of the HUCs. The x-intercept value at high frequency region in the Nyquist plot indicates the resistance value, shown in Fig.7. Response time is another important parameter of HUCs which can be estimated from bode plot (phase vs. frequency) using A. C. impedance spectroscopy. In Bode plot the resistance and capacitive reactance are equal at  $-45^\circ$  phase angle; the corresponding frequency called as

breaking frequency. Beyond this frequency capacitive reactance become larger than resistance. The time corresponding to the breaking frequency is represented as response time of the capacitor. The response times for the HUCs are estimated to be 1.66 s and 4.68 s for the AGM and gel electrolyte configurations, respectively shown in Fig.8 (a, b). These lower response times indicate the effective pulse power applications of the HUCs.

#### *Energy density and power density calculations*

Battery is recognised as an energy device and capacitor as a power device. But as substrate-integrates lead-carbon HUC devices are overarch of these two, the energy density and power density are the curtail components for its applications. These two are estimated from the constant power discharge profiles of HUCs. Energy values can be calculated from discharge plots by the multiplication of the discharge times and the corresponding powers. Energy density is the normalised form of calculated energy by the total weight of HUCs. To calculate the power density the response time is an important factor that can be known from the impedance study. Power density is nothing but the ratio of energy density and the response time. The energy and power densities of HUCs are summarized in Table 1.

#### *Self-discharge, leakage current and parallel resistance measurement*

In the present study, self-discharge for the HUCs was measured after charging them potentiostatically for 3h at 13.8 V followed by 24 h in open-circuit condition at room temperature (28°C ) and 50°C shown in Fig 9 (a, b). It is observed that at higher temperature, the self-discharge is only marginally increased. Self-discharge data accumulation was also conducted for seven days at room temperature shown in Fig 9 (c). 'Self-discharge energy loss factor (SDLF)' was calculated from the voltage loss data with respect to time according to the following equation.

$$(\text{SDLF}) = 1 - (V/V_w)^2$$

Whereas  $V$  and  $V_w$  are the voltage after measured time and the working voltage [8]. Self-discharge for the gelled configuration is higher than the AGM configurations. As the self-discharge is higher for gelled system, the leakage current also is higher while parallel resistance is lower for it. Leakage current was measured during 24 h after fixing the voltage at 13.8 V. Parallel resistance after 24 h was obtained as a ratio of working voltage, i.e. 13.8 V, and leakage current after 24 h. Self-discharge, leakage current and parallel resistance values for AGM and gelled HUCs are given in Table 2. It is noteworthy that the enhancement in active surface area of  $\text{PbO}_2$  active material is ads up to self-discharge of HUC in gel configuration.

#### *Pulse- cycling data*

12 V substrate-integrated lead-carbon HUCs were subjected to pulsed cycle-life test under charge-discharge current load of 30 A, at first 50,000 cycles for duration of the 1 s followed by rest for 5 s. The effect of high-rate pulsed cycling on the capacitance of these HUCs was also studied. 50,000 cycling with 60 A charge-discharge pulse rates for 1 s followed by 10 s rest were also performed. The capacitance measurements were carried out at 3 A current discharges after each 10,000 cycles and data are shown in Fig. 10. After 100,000 cycles the capacitance loss are calculated as 36 % and 23 % for AGM and gelled HUCs respectively. The enhanced cycle-life of the HUCs are mainly attributed for the coupling of the capacitor electrode with the battery type electrode. This data is truly attractive for the long term applications of HUCs.

**Table 1.** Energy density and power density data for AGM and gelled HUCs.

	<b>Energy Density</b> / Wh kg <sup>-1</sup>	<b>Response Time</b> / s	<b>Power Density</b> / W kg <sup>-1</sup>
<b>AGM</b>	0.9	1.66	1937
<b>Gel</b>	1.8	4.86	1333

**Table 2.** Self-discharge, leakage current and parallel resistance data for AGM and gelled HUCs.

<b>Parameter</b>	<b>AGM</b>	<b>Gel</b>
<b>Self-discharge at room temperature for one day (28 °C) / %</b>	15	18
<b>Self-discharge at 50 °C for one day / %</b>	19	22
<b>Self-discharge at room temperature for seven days (28 °C) / %</b>	23	26
<b>Leakage Current / mA</b>	80	180
<b>Parallel Resistance / Ω</b>	173	77

## Figure captions

**Fig. 1.** Photograph of a 12V/kF-range LC HUC.

**Fig. 2:** Constant current discharge profiles at varying current loads (3, 6, 9, 12, 15A) (a) AGM, (b) gelled HUCs.

**Fig. 3:** Constant current discharge profiles at varying current loads (25, 50, 75, 100A) (a) AGM, (b) gelled HUCs.

**Fig. 4:** Capacitance study at variable temperatures for (a) AGM, (b) gelled HUCs.

**Fig. 5:** Constant current charge-discharge profiles of HUCs.

**Fig. 6:** Constant power discharge profiles at varying power loads (a) AGM, (b) gelled HUCs.

**Fig.7:** Resistance vs. potential profiles for HUCs. Inset: Nyquist plots of AGM and gelled HUCs.

**Fig. 8:** Response time measurement plots for (a) AGM, (b) gelled HUCs.

**Fig. 9:** Self-discharge profiles of HUCs (a) one day at room temperature, (b) one day at 50 °C, (c) Seven days at room temperature; Inset: Percentage of voltage loss vs. time plot.

**Fig. 10:** Cycle life test data for HUCs.



**12V / kF-range Lead-Carbon HUCs**

Fig. 1

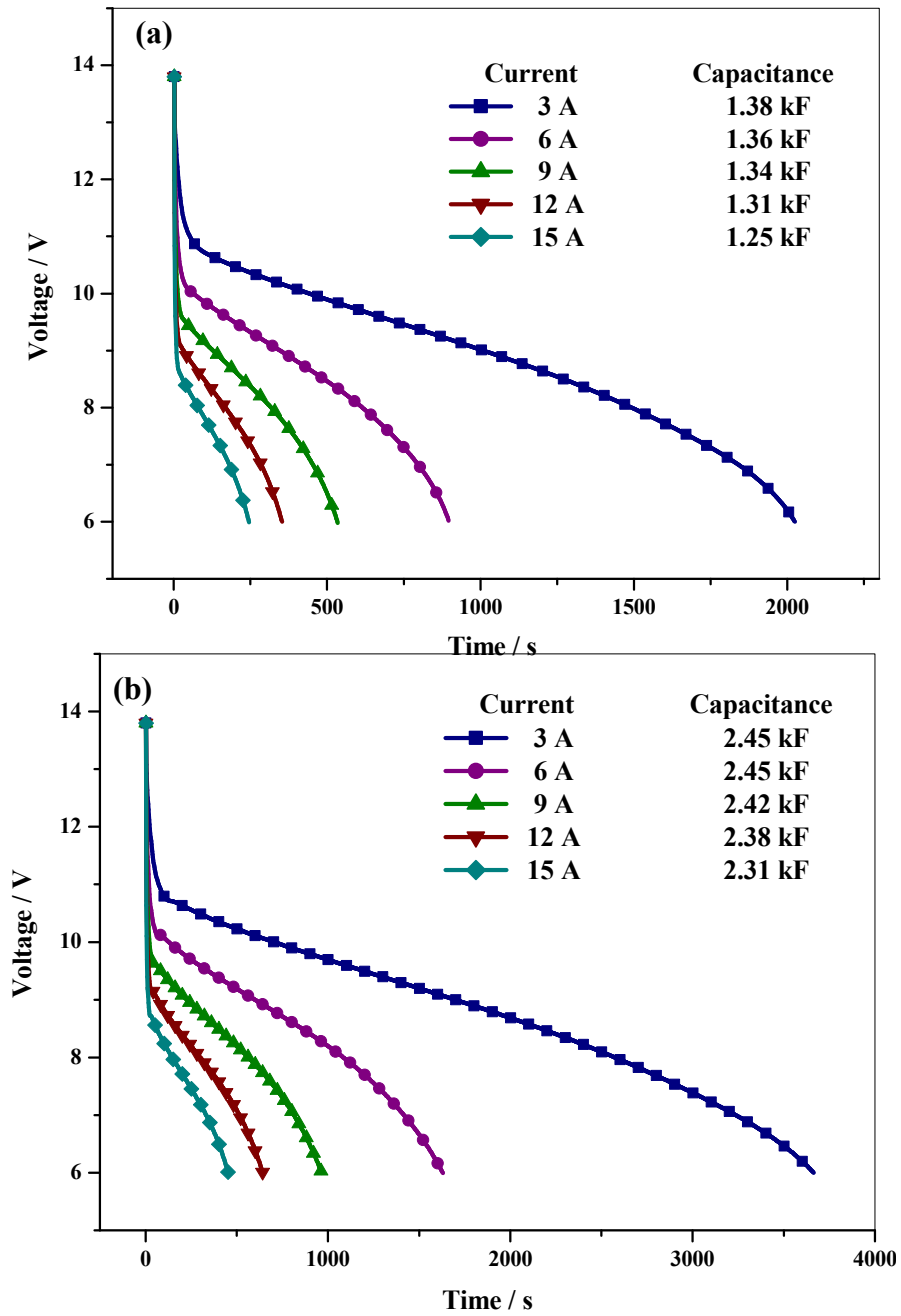


Fig.. 2

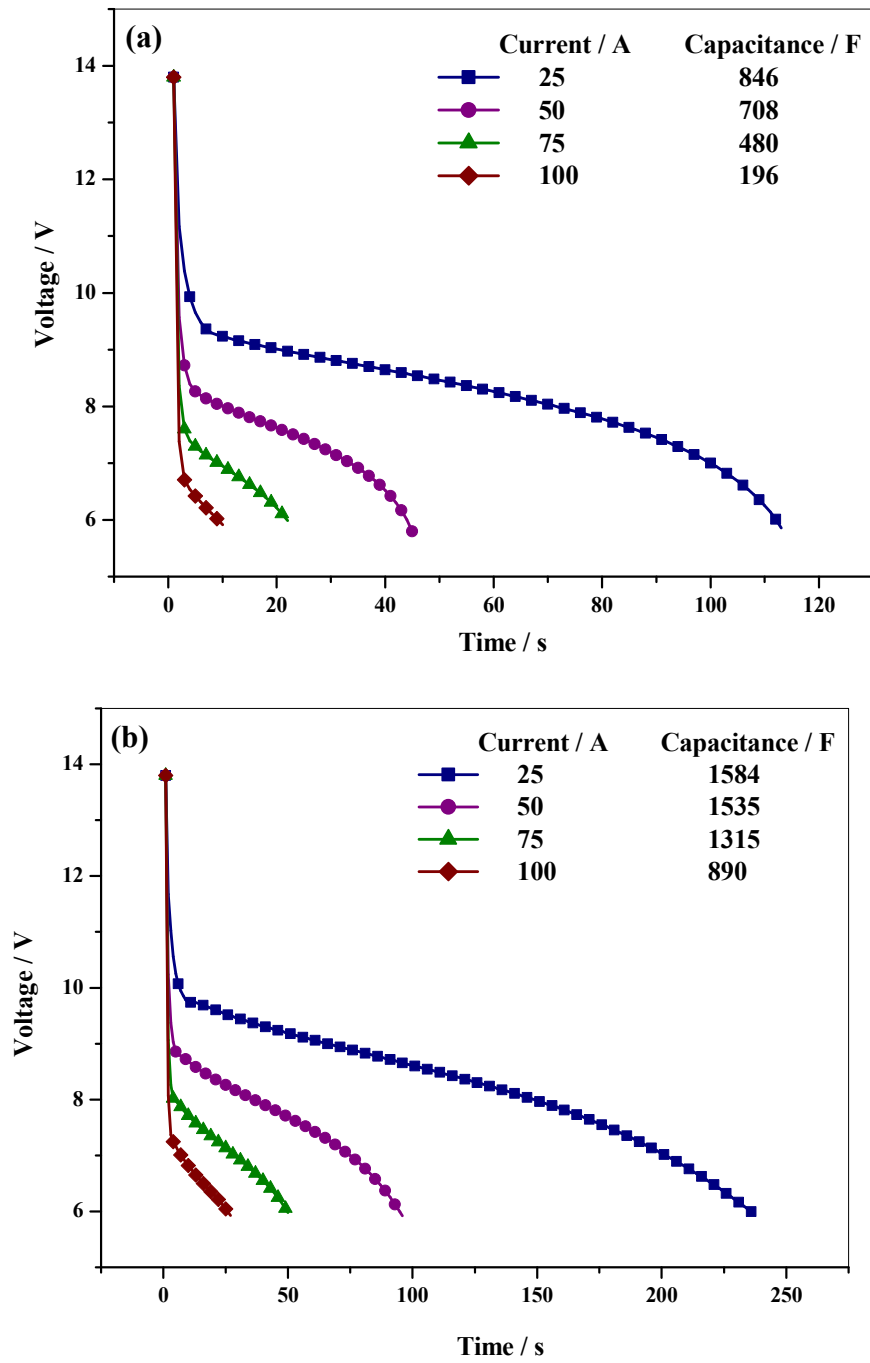


Fig. 3

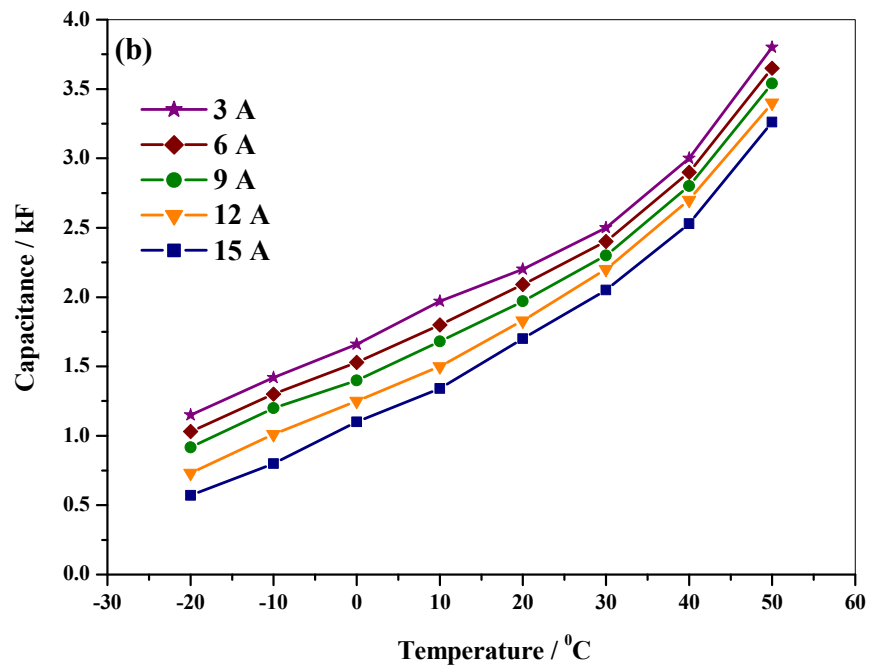
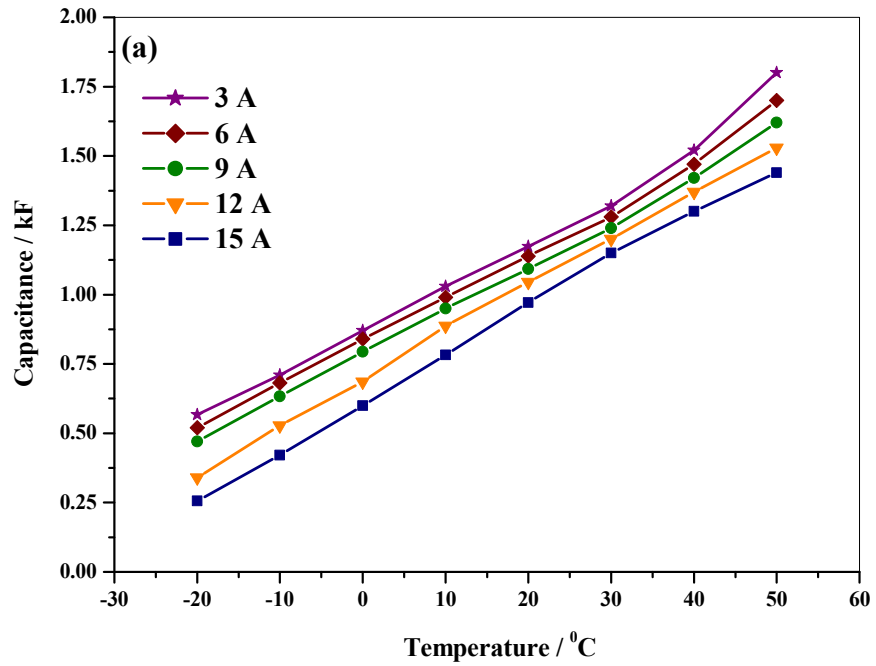


Fig. 4

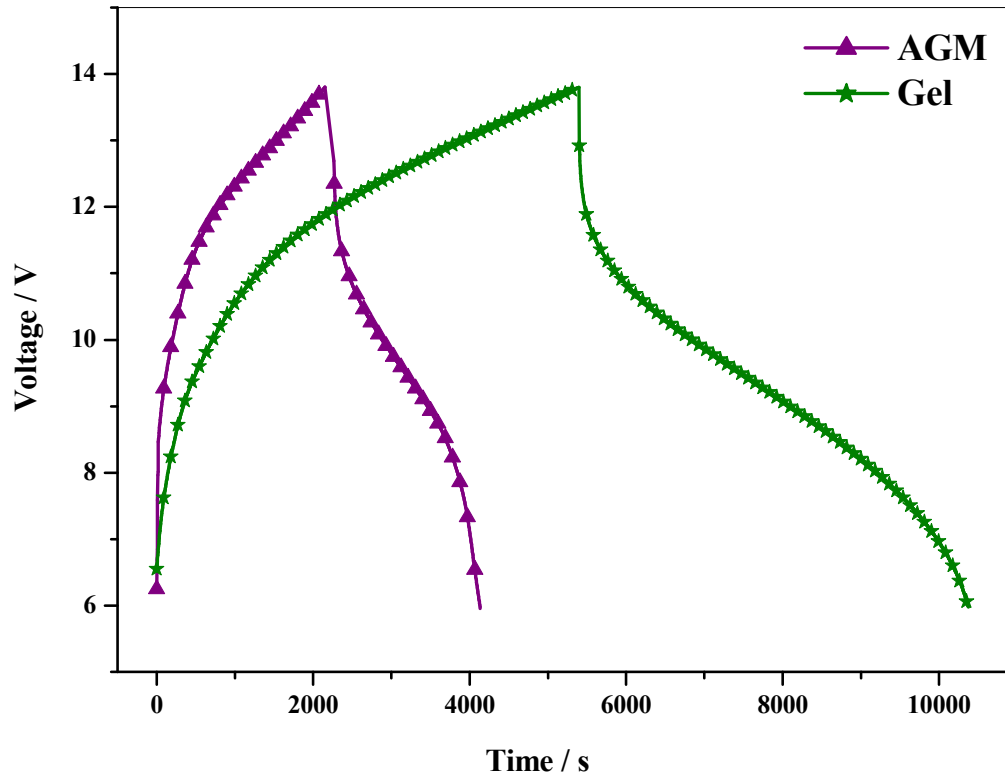


Fig. 5

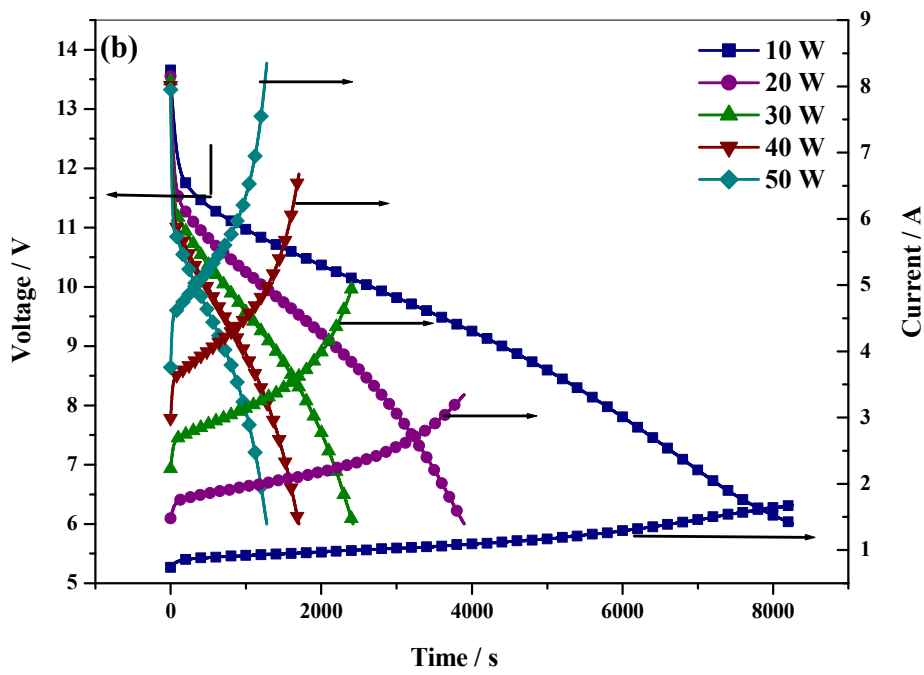
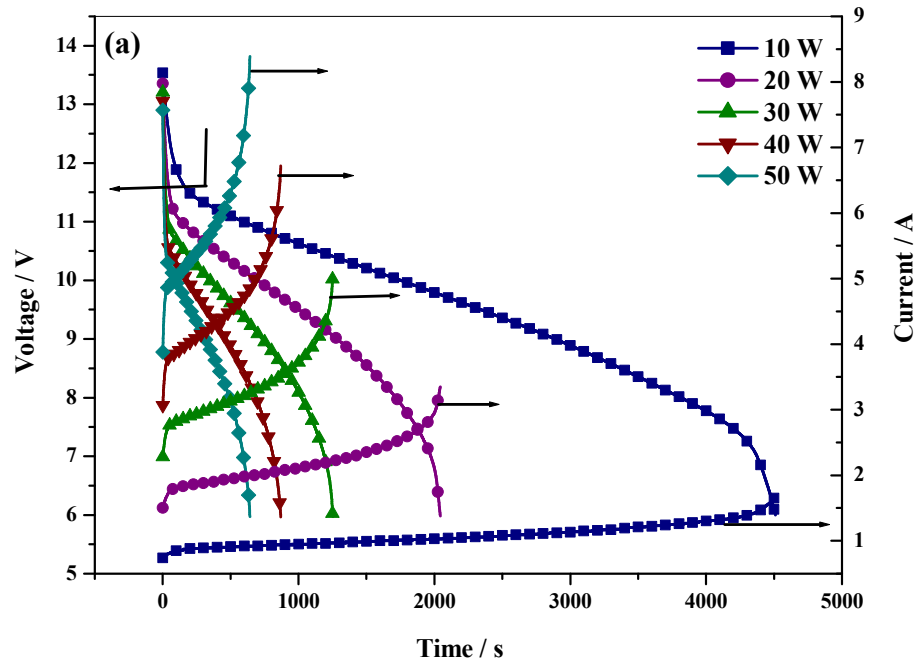


Fig . 6

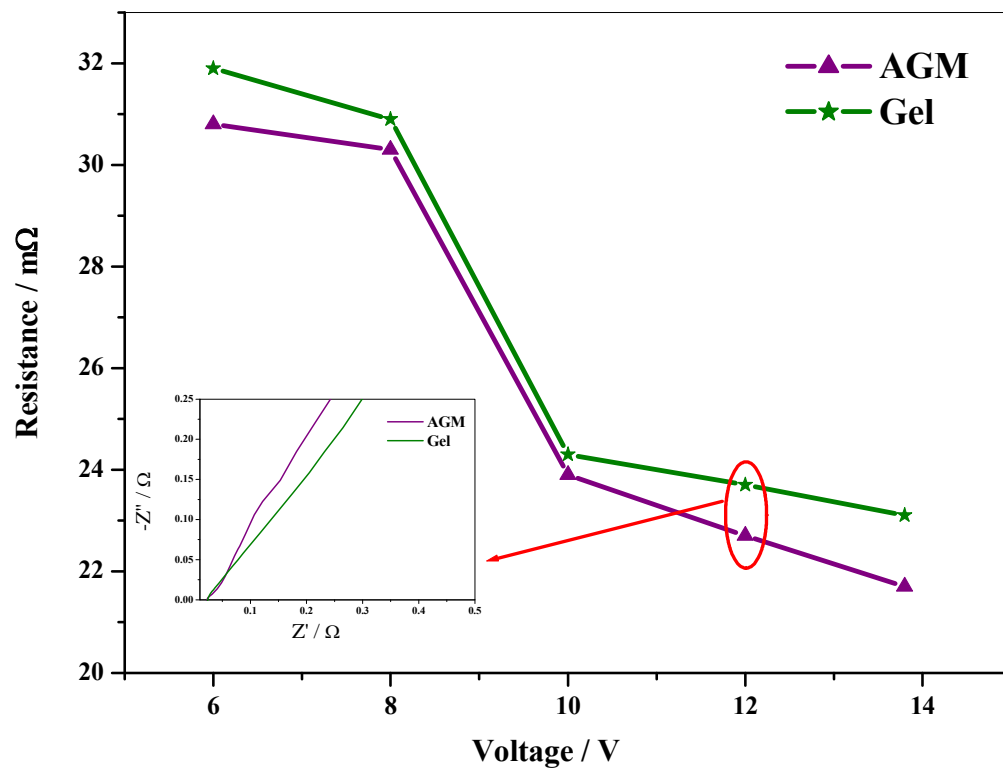


Fig. 7

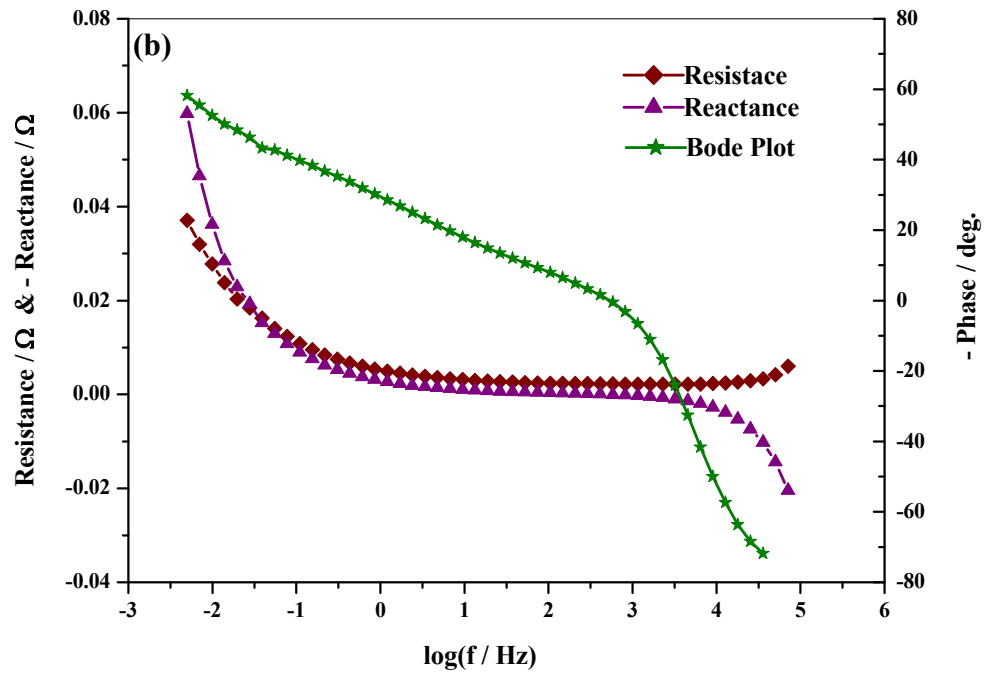
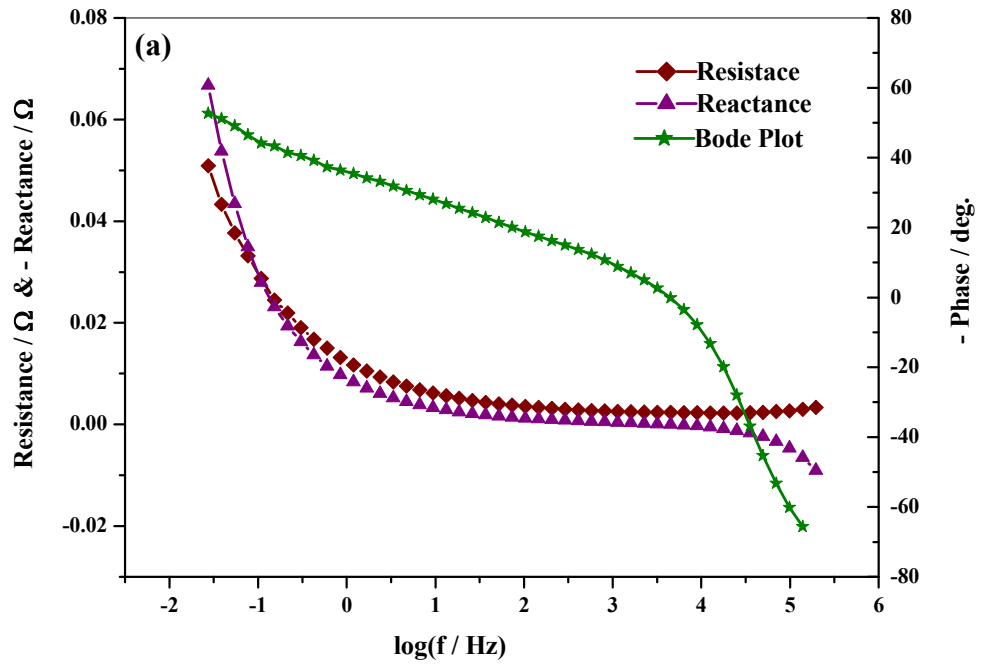


Fig. 8

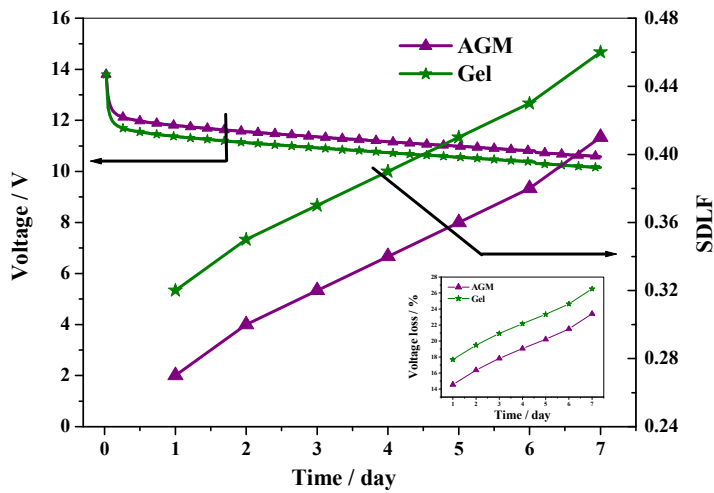
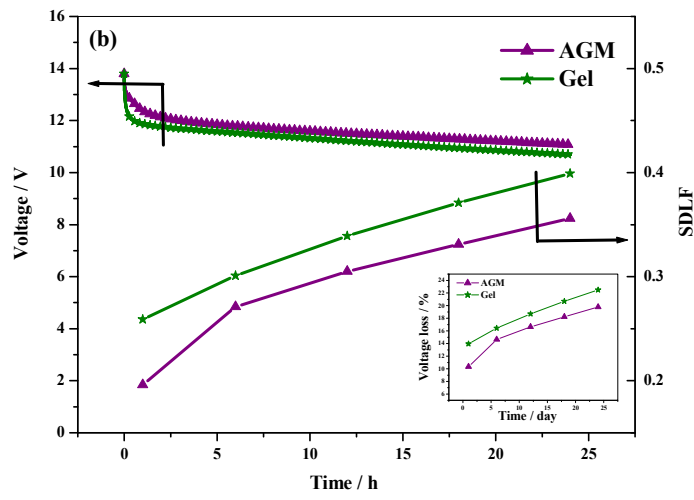
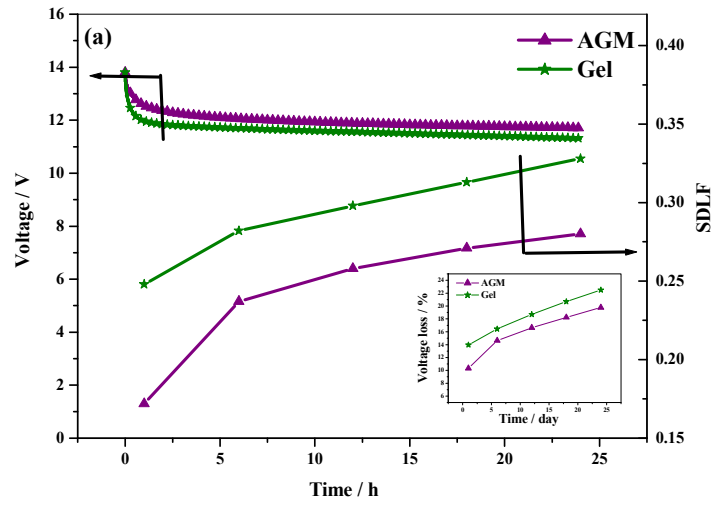


Fig. 9

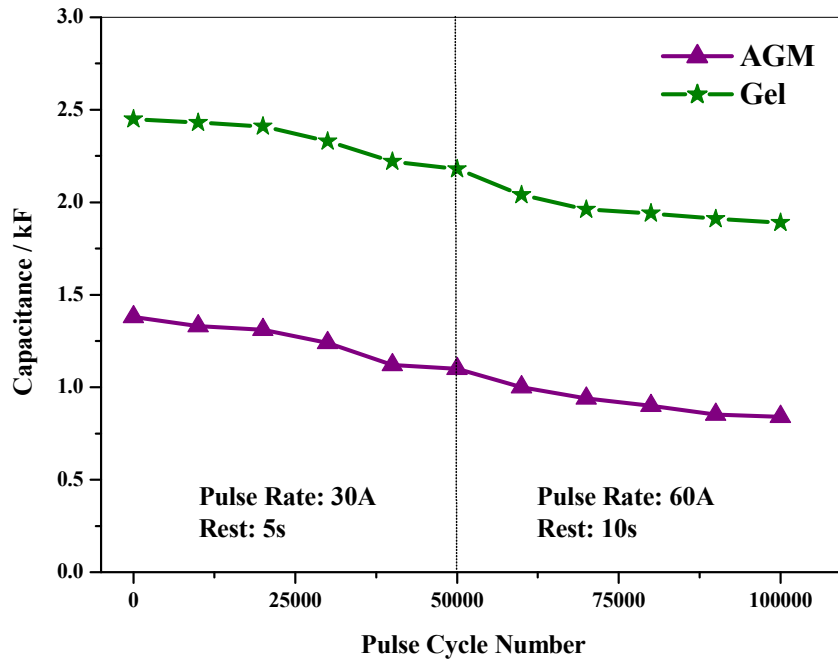


Fig. 10